J Mater Sci (2009) 44:469–476
DOI 10.1007/s10853-008-3094-z

Investigations of a controllable nanoscale coating on natural fiber system: effects of charge and bonding on the mechanical properties of textiles

C. Yang · P. Gao · B. Xu

Received: 18 August 2008 / Accepted: 29 October 2008 / Published online: 23 November 2008

Abstract A novel nano-sized copolymer nanofilm provides a unique reinforcement to the mechanical properties of natural textiles. This study reveals that a nano-sized coating provides a strong healing effect to resist the crack propagation of natural fiber surfaces. As little as 0.15 wt% addition of the nanoparticles to the cotton surface improved the fabrics' tearing resistance by 56% and abrasion resistance by 100%. Surface analyses (SEM and AFM) demonstrated that the nanoparticles formed a uniform monolayer and after heat treatment the monolayer nanofilm covalently bonded to the substrate. This nanofilm is reliable in repeated washes due to its covalent bonding. Using time-of-flight secondary ion mass spectroscopy (TOF-SIMS), we studied the reactivity and phase-transition process of the nanoparticles as they transformed into the nanofilm. The study demonstrates the active role of the *N*-methylol group and the primary hydroxyl group toward the cotton surface, which modulate the rupture process of the fiber substrate; meanwhile, it demonstrates the positively charged nanoparticles have an excellent dispersibility on the negatively charged cotton surface. The result opens the possibility for various textiles to enhance their properties via an electrostatic affinity and covalent bonding of functional nanoparticles.

Electronic supplementary material The online version of this article (doi:10.1007/s10853-008-3094-z) contains supplementary material, which is available to authorized users.

C. Yang · B. Xu
Department of Chemistry, The Hong Kong University of Science and Technology, Clear Water Bay, Hong Kong, China

P. Gao (✉)
Department of Chemical Engineering, The Hong Kong University of Science and Technology, Clear Water Bay, Hong Kong, China
e-mail: kepgao@ust.hk

Introduction

Currently there is an urgent need for new multifunctional textiles with performances that exceed the traditional textiles for medical, military, and other specialty applications [1–7]. Inorganic coating methods including sol-gel and solution immersion have been studied for surface finishing of textiles, but they encounter a few restrictions in specific applications, such as their low resilience, a large demand of energy, and creating lots of wastes [8–11]. Recently, the application of polymeric nanoparticle emulsions for functionality enhancement of cellulose-based fabrics is being noticed. For example, Soane et al. [12] developed a payload method to functionalize the textile surface with polymeric encapsulators through a covalent bonding, therefore ensuring the capability of controlled-release of a variety of chemicals to the textiles. Alince et al. [13, 14] reported their studies using polymeric latex for paper treatment and observed enhancements in their tear resistance, tensile resistance, and elongation at break. Studying the controllable nanoscale coating using the polymeric materials on various fabrics and textiles opens a new horizon in improving the material performances for new applications and significantly broadens the scope of the early traditional textile materials for new or enhanced systems.

N-hydroxymethyl acrylamide (NHMAm) bears the typical *N*-methylol group which has a strong reactivity to cellulose. It can be polymerized and the polyNHMAm has strong bonding ability toward cellulose under Lewis acid

catalysis [15]. In a durable press (DP) treatment process, the polyNHMAm can couple with the resin (dimethylol-4, 5-dihydroxylethyleneurea (DMDHEU)) and bind to the cotton surface via a same mechanism as DMDHEU does. In this work, we compiled the reactive polyNHMAm with other thermal elastic polymers and prepared nanoparticles with both sufficient reactivity and mechanical strength, and observed its efficiency in the enhancement of the mechanical property of the fabrics. We also characterized the film formation property and the phase-transition process of the nanofilms formed by the nanoparticles, and analyzed the efficiencies in various conditions.

Based on a large amount of experimental explorations, we selected the seeded emulsion polymerization method and prepared the polystyrene-co-butylacrylate-co-*N*-hydroxymethyl acrylamide-co-hydroxyethyl methacrylate-co-vinylbenzyl trimethylammonium chloride nanoparticles (NP1) [16]. To eliminate the contamination from small molecular surfactants and to enhance the colloidal stability of the emulsion, we used vinylbenzyltrimethyl ammonium chloride (VBTMAC) as an amphiphilic monomer to adjust the electrostatic property of NP1, because VBTMAC can improve the stability of the electrical double-layer structure of the emulsion to the environments, compared to using other small molecular surfactants [17–19]. When coupled with seeded emulsion polymerization, it is more efficient in forming smaller size of latex colloids than using other small molecular surfactants [19]. Meanwhile, the positively charged VBTMAC functional group enables the emulsion nanoparticles more easily to adhere to the negatively charged cotton surface [14, 20]. Using reactive surfactant monomers can also reduce the amount of small molecules in the emulsion such as surfactants and unreacted monomers. On the other hand, we used *N*-hydroxymethyl acrylamide (NHMAm) and hydroxylethyl methacrylate (HEMA) to enhance the reactivity of the nanoparticles toward cellulose. The *N*-methylol group and the primary hydroxyl group can make the nanoparticles readily react with both DMDHEU and cotton cellulose via a dehydration process at elevated temperature [21, 22]. Results obtained from this study provide information about the surface interaction between the polymeric emulsion nanoparticles and the fiber substrates, which is useful to understand the failure mechanism of fiber and to design advanced nanocoatings for natural materials.

Materials and methods

Materials

All chemicals were obtained from Aldrich. 2,2′-azobis (2-amidinopropane) dihydrochloride (V50) and potassium persulfate (KPS) were used as received. Magnesium sulfate 6-hydrate ($MgCl_2$) was obtained from Fluka. *N*-hydroxymethyl acrylamide (NHMAm) was obtained from Wako Pure Chemical Industries (Osaka, Japan). Deionized water was distilled to have an electric resistance higher than 180 kΩ m.

Preparation of nanoparticles

The preparation of nanoparticles follows the method of seeded emulsion polymerization [23–26]. The polymerization was conducted in a 2-liter fermenter reactor equipped with four baffles and six-blade pitched paddle impeller. The width of the baffles was 1 cm, and the diameter and width of the impeller were 5 and 1 cm, respectively. The impeller was located at one-third of the liquid height from the bottom. The polymerization protocol is described below: Firstly, the aqueous solution of seed monomers was deoxygenated by bubbling with nitrogen for 30 min under stirring. Secondly, the reactor was heated to 50 °C using circulating water jacket, and the initiator solution (V50) was added to the reaction mixture to initiate polymerization. It was heated until the temperature reached 67 °C at a heating rate of 1 °C/min, then the mixed monomers were dropped in at a rate of 40 mL/h using a dropping funnel. The temperature was kept constantly for 5 h, then the reaction was stopped by reducing the temperature to room temperature gradually. All runs were conducted under a nitrogen atmosphere at an impeller speed of 350 rpm.

Characterizations of nanoparticles

1. The nanoparticle samples were spin-coated on silicon wafers and characterized on a digital instruments scanning probe microscope-nanoscope atomic force microscope (AFM). 2. Scanning electron microscopy (SEM) (Model: JEOL 6700F) was used to investigate the morphology of the fabric samples after coating with the nanoparticles. 3. The hydrodynamic size-distribution of the emulsions was analyzed on a dynamic laser light scattering workstation (Precision Detectors PD2000/DLS). 4. The nanoparticles (NP1) were spin-coated onto silicon wafers and dried at ambient temperature. The wafers were heated and kept for 10 min at the temperatures of 80, 110, 140, and 180 °C, respectively. AFM analysis was carried out on these heat treated nanoparticles with tapping mode in order to study the phase transition of the polymer domains after treatment at different temperatures. 5. TOF-SIMS measurements were performed on a Physical Electronics PHI 7200 TOF-SIMS spectrometer. The chemical spectra of the nanoparticles were acquired in the negative mode using a Ga^+ liquid metal ion source operating at 25 keV. The total ion

Table 1 Formulation of the polymerization of NP1

Initial composition	
S	6.55×10^{-5} mol
NHMAm	3.96×10^{-2} mol
VBTMAC	1.66×10^{-2} mol
V50	1.38×10^{-2} mol
Additional component	
S	6.98×10^{-4} mol
BA	3.14×10^{-4} mol
HEMA	8.24×10^{-5} mol

dose was lower than 4×10^{12} ions/cm^2 in a high vacuum of 1.5×10^{-9} Torr. Besides the heat treatment of the nanoparticle samples on silicon wafers, we also analyzed the morphology of the NP1 samples coated on native cotton fabric (1 cm^2). These fabric samples were heated and kept for 10 min at the temperatures of 80, 110, 140, and 180 °C, respectively. 6. Zeta potential of the nanoparticles at different pH values was analyzed using a Delsa™ 440SX Zeta Potential Analyzer. In the test, the nanoparticles were diluted into a NaCl solution (0.01 M), HCl and NaOH were used to adjust the pH value. All measurements were made on dispersions that had been equilibrated for 24 h at the appropriate pH. NaCl was used as the reference electrolyte in the analysis (Table 1).

Fabric treatment process for mechanical property evaluations

An aqueous solution (500 mL) containing 18 v/v% DMDHEU, 1.2 wt% $MgCl_2$, 8 v/v% softeners (4% siloxane, 4% PE-siloxane), and NP1 (0.15–0.6 wt%) were well dispersed together with deionized water (DI water). (The condition listed here ensures the treated fabric achieve wrinkle resistance rating over grade 3.5 of total 5 grades.) Five pieces of textile samples (300×200 mm^2) were dipped in the bath of the suspension, and then rinsed gently for 7 min. Then the textile samples were picked up and padded at 15 kg/cm^2 to achieve a wet pickup of 80 wt%. Afterwards, the samples were placed into a tumble dryer (ZANUSSI TD-892N) and dried at 60 °C for 7 min to achieve a wet-pickup of 25%. Then the samples were hand-ironed at 110 °C to remove wrinkles before they were clamped with four stationary clamps between two pieces of glass plates ($300 \times 200 \times 3$ mm^3) and cured at 145 °C for 6.5 min in a Memmert ULE500 oven.

Mechanical property testings of the fabric samples

The procedures for testing followed general methods for DP fabrics. Tear and tensile testings were based on six specimens; abrasion test was based on two specimens. Strips cut from the fabric samples after DP rating were used to measure breaking strength (ASTM D 1682-64; Instron Tester, crosshead speed = 10 in/min), tearing strength (ASTM D 1424-63; Elmendorf Tear Tester, 1,600 g weight, abrasion (ASTM D 1175-64; Universal Wear Tester), durable-press rating (5 grades) (AATCC Test Method 124-1969), and wrinkle recovery in the weft direction (ASTM D 1295-67; Monsanto Tester. 500 g weight) [27–29]. All testings were carried in a closet with air-conditioning system at 21 ± 2 °C with the relative humidity of 65 ± 2% for equilibrium. (All data were based on weft direction.)

Results and discussion

Size distribution of the nanoparticles

As one of the major concerns of the study, the colloidal stability of the nanoparticles was demonstrated by using light scattering method. The concentration of the electrolyte of $MgCl_2$ in this study was 12 g/L to simulate a real dipping condition. After mixing the nanoparticles in the $MgCl_2$ solution for 8 h, the NP1 emulsion was analyzed with dynamic light scattering. Test results showed that NP1 were quite stable in the $MgCl_2$ solution after 8 h (Fig. 1). This showed that NP1 was well dispersed in the catalyst solution long enough for commercial cycling dipping process of the DP treatment. In addition, we observed that NP1 performed good dispersibility in the DMDHEU-$MgCl_2$ solution for DP treatments.

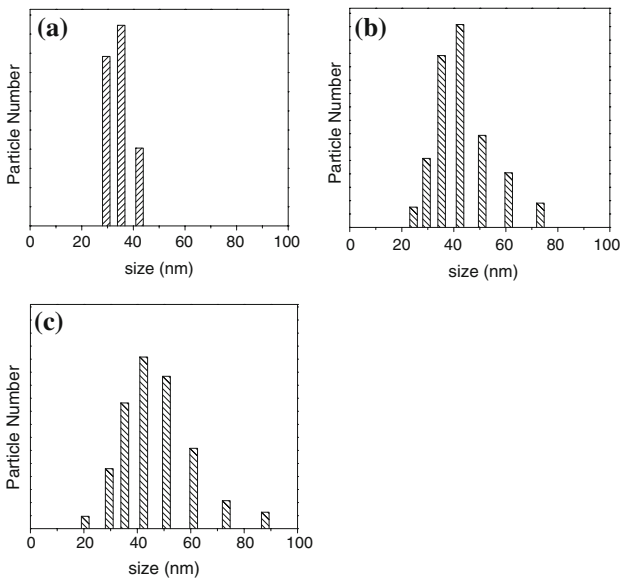

Fig. 1 Particle size distribution of the NP nanoparticles in **a** distillated water, **b** 12 g/L $MgCl_2$ solution, **c** 15% DMDHEU and 12 g/L $MgCl_2$ solution

Phase-transition and functionality of the nanoparticle films under different temperatures

The surface functionality of the nanoparticles at elevated temperature is crucial for the efficiency of the fabric treatment process. However, the phase transition process of the copolymer at elevated temperature may affect the reactivity of the surface functional groups [30]. In order to characterize the surface functionality of NP1 upon film formation stage after deposition onto the fiber surface, we analyzed the nanoparticles using TOF-SIMS after different thermal treatments. The samples were loaded on two different surfaces: one was to test the nanoparticles on silicon wafer (silicon wafer substrate also facilitates the analysis in their morphology using AFM (Fig. 2)). The other group was applied on the cotton fabric surface which represents a more realistic situation for practical uses (Table 2). In addition, we also used native cotton fabric sample as a control for TOF-SIMS analysis. In the TOF-SIMS spectra, we studied the major characteristic peaks at m/z 42, 45, 57, and 91. The characteristic troplium cation $C_7H_7^+$ peak (m/z 91) which originated from

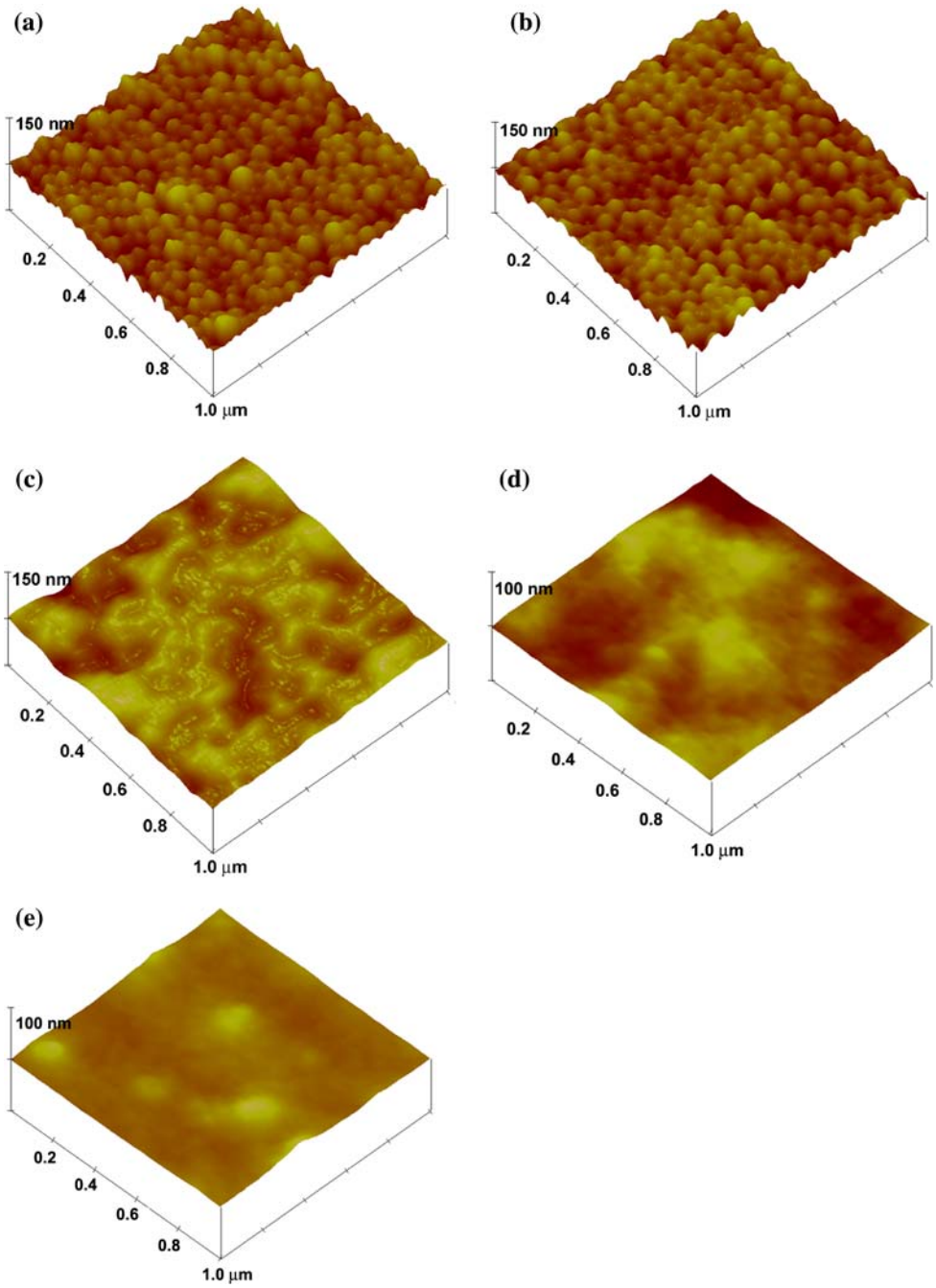

Fig. 2 AFM analysis of the nanofilm of NP1 (dried at room temperature). **a** original NP1 film, **b** NP1 film heated to 80 °C for 10 min, **c** NP1 film after heating to 110 °C for 10 min, **d** NP1 film after heating to 140 °C for 10 min, **e** NP1 film after heating to 180 °C for 10 min

Table 2 TOF-SIMS analysis of the NP1 nanoparticles

(Relative intensity)	$C{=}ON^+$ (m/z 42)	$C_2H_5O^+$ (m/z 45)	$C_4H_9^+$ (m/z 57)	$C_7H_7^+$ (m/z 91)
	NP1 nanoparticles			
25 °C	0.099 ± 0.004	0.207 ± 0.017	0.271 ± 0.018	1
140 °C	0.029 ± 0.001	0.032 ± 0.001	0.334 ± 0.001	1
	NP1 nanoparticles on cotton fabric surface			
25 °C	0.115 ± 0.013	0.250 ± 0.011	0.644 ± 0.107	1
140 °C	0.066 ± 0.001	0.183 ± 0.005	0.415 ± 0.002	1
	Native cotton			
25 °C	0.043 ± 0.006	0.196 ± 0.012	0.165 ± 0.020	0.021 ± 0.002

polystyrene (PS) was used as a reference to illustrate the intensities of other peaks (relative intensity was termed 1 in all samples except for native cotton). The relative intensities of all other peaks over it were used to indicate the relative abundance of the functional groups at the surface corresponding to the rise of temperature. $C_4H_9^+$ (m/z 57) is the characteristic peak for the component of polybutyl acrylate (PBA). PBA is a hydrophobic polymer with very low glass transition temperature. PBA region has the highest relative intensity to $C_7H_7^+$ when temperature is at 140 °C. The characteristic peak for polyhydroxylethyl methacrylate (PHEMA) domain ($C_2H_5O^+$, m/z 45) decreased drastically from approximately 21% to 3% when temperature was raised from 25 °C to 140 °C. However, on cotton, the relative intensity of the same fragment ($C_2H_5O^+$) decreased from 25% to 18% when the temperature was raised from 25 °C to 140 °C. These results reflect that the cotton surface has the ability to inhibit the phase transition of the nanoparticles. This phenomenon shows that the nanoparticles may have even higher reactivity on cotton fabric at 140 °C, which is the temperature for the DP curing process. The fragment of $C{=}ON^+$ (m/z 42) may originate from both NHMAm and VBTMAC. The intensity of this cation did not show much difference at the temperature of 140 °C on different substrates (silicon wafer and cotton). This test proves that the NP1 nanoparticles have reactivity toward both cellulose and resin during the fabric curing treatment.

Topological analysis of the nanoparticles under different temperatures

In addition to the functionality analysis of NP1 at different temperatures, we also observed the topological features of the dried NP1 films using atomic force microscopy (AFM) at the corresponding temperatures of TOF-SIMS studies. At 25 °C (Fig. 2a), the spherical structure of the nanoparticles remained intact. We observed that the surface topology of the nanoparticles was not as sharp as before the heat treatment, when we raised the temperature and retained it at 80 °C (Fig. 2b) for 10 min before scanning. This morphological change indicated that at 80 °C only minor phase-transition took place at the surface of the nanofilm. We observed that the nanoparticles merged into a film with rippled texture at the surface when the temperature was raised and retained at 110 °C (Fig. 2c) for 10 min before AFM analysis. Then we further raised the temperature until 140 °C and 180 °C (Fig. 2d, e), which are the temperature over glass transition temperature (T_g) of most of the polymer chains involved. We observed that the surface of the nanofilm became much flatter as the temperature increased.

Surface morphology of the nanoparticle treated fiber samples

In order to analyze the dispersibility of NP1 on cotton fiber surface, we carried out SEM analysis and used three other kinds of nanoparticles as the control; they are: sodium styrenesulfate emulsified nanoparticles (NP2), sodium dodecylsulfate emulsified nanoparticles (NP3), and cetyltrimethylammonium bromide emulsified nanoparticles (NP4) [27]. Compared with NP1, these control samples have similar particle size and composition, but they are different in the surfactant molecules in use. Figure 3 displays the SEM images showing NP1 and NP2 nanoparticles treated fabric samples. The NP1 nanoparticles were able to form a uniform nanofilm on cotton surface (Fig. 3a, c); after heat treatment, the fiber surface was evenly covered with the nanoparticles (Fig. 3e). However, the NP2 nanoparticles showed inferior coverage on cotton fiber surface because of the agglomerations (Fig. 3b, d). They covered limited regions of the fiber surface, and formed lumps and stuck the adjacent fibers (Fig. 3f). This was resulted from both the mutual negative charge with fiber and the weak stability in the $MgCl_2$ solution. All these three types of control nanoparticles showed inferior efficiency in film formation on cotton compared to the NP1 nanoparticles.

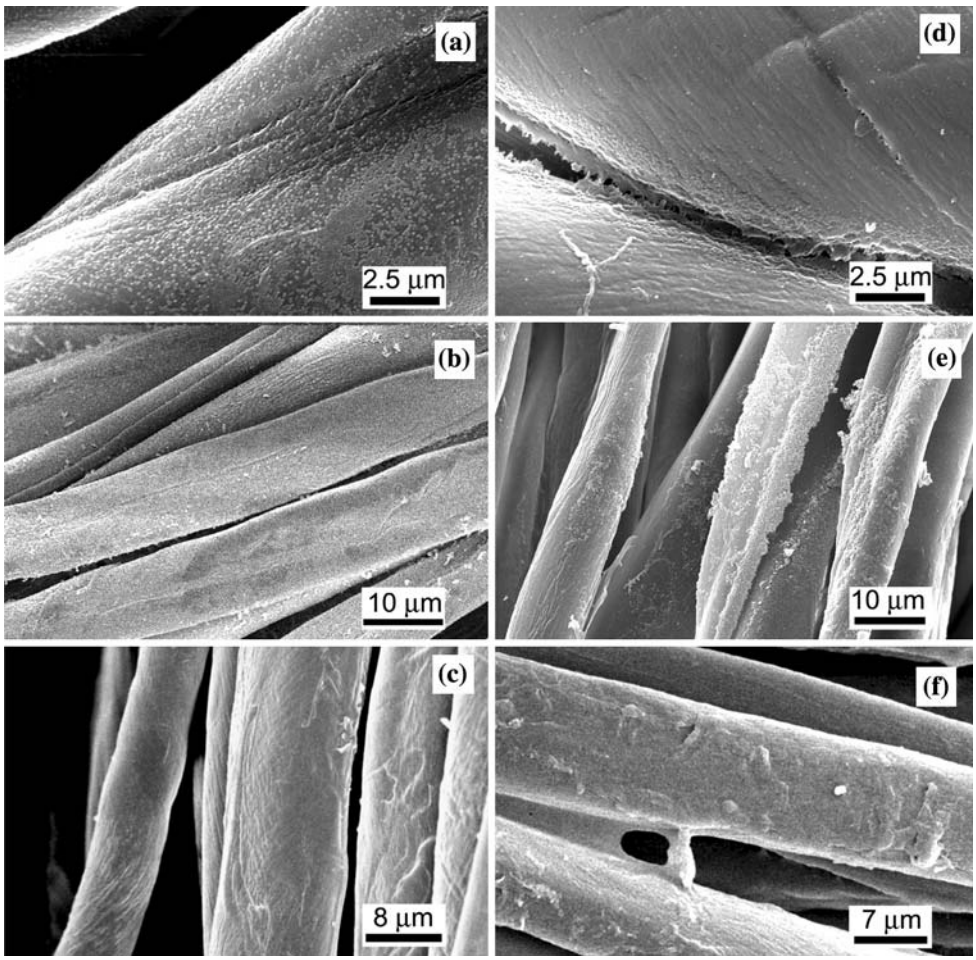

Fig. 3 SEM analysis of fabric samples after a resin treatment process. **a**, **b** are: high and low magnification SEM images of NP1-resin treated fabric, **c** NP1-resin treated fabric after curing step. **d**, **e** are: high and low magnification SEM images of NP2-resin treated fabric, **f** NP2-resin treated fabric after curing step. The concentration of each nanoparticles emulsion is 0.15 wt%, DMDHEU is 15 wt%, and $MgCl_2$ is 12 g/L. Curing condition: 145 °C for 6.5 min

The mechanical testing experiments of the cotton fabric samples using these three control nanoparticles all showed worse results compared with the NP1 nanoparticles.

Discussion about the interface mechanism of the nanoparticles and fabrics

Cotton fiber is biologically composed of the primary wall, the secondary wall, and lumen [31]. As the major part, the region of the secondary wall has a highly oriented, spiral microfibril structure, which shows much higher crystallinity than the primary wall; therefore, the axial stress between the adjacent microfibrils can be easily transferred from one to another [31]. As for the primary wall (outer region), the cellulose is primarily in amorphous phase; after DP treatment, it turns from a soft, flexible form into a rigid, brittle, and crosslinked one. Therefore, during the surface abrasion or fabric shearing, the crosslinked fiber surface ruptures easily and this results in peeling damage [32, 33]. The positively charged, reactive NP1 nanoparticles can absorb evenly onto the cotton fiber surface through a dipping process, and they formed a single layer at the fiber surface. After the curing process, this thin layer gets into a uniform nanofilm which covalently bonds to the fiber surface. This thin film functions as a protecting jacket to modulate the initiation step of the surface rupture and remedy for the surface fatigue to enhance the shear resistance of the DP cotton fiber (Scheme 1). Moreover, because the NP1 nanoparticles' dry pickup is at very low percentage ($\sim$0.01 wt%) and the nanofilm evenly coats the

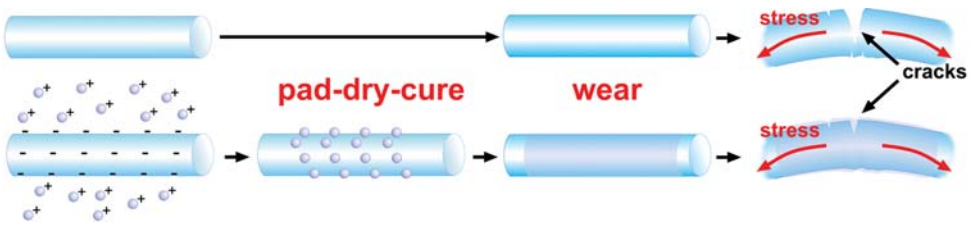

Scheme 1 Illustration of the treatment process of the fiber and the function of the coating material

Table 3 The crease-recovery property and the mechanical properties of the NP1 treated textile samples at different temperatures and NP1 concentrations

Mechanical performances of NP treated fabric samples				
	Tear (N)	Tensile strength (MPa)	Dry recovery angle (°)	Abrasion (×1,000 cycles)
Cured at 140 °C				
0.15%	10.97 ± 1.87	34.09 ± 1.53	141.5 ± 3.1	38.5 ± 2.1
0.30%	11.88 ± 0.25	35.19 ± 0.66	141.3 ± 2.9	27 ± 8.5
0.60%	12.19 ± 0.26	34.85 ± 1.51	137.5 ± 1.3	38 ± 6.0
Control	8.45 ± 0.25	33.31 ± 1.01	141.8 ± 1.3	19 ± 1.5
Cured at 145 °C				
0.15%	11.09 ± 0.15	33.21 ± 0.45	143.0 ± 0.8	27.0 ± 12.5
0.30%	10.38 ± 0.77	32.65 ± 0.35	143.8 ± 1.0	33.5 ± 2.0
0.60%	11.01 ± 0.68	34.21 ± 1.73	144.8 ± 1.0	21.5 ± 2.0
Control	7.05 ± 0.31	30.67 ± 1.28	145.5 ± 1.3	15.5 ± 0.5

fiber surface, the effect to hand feel and water-absorbance of the fabric can be negligible.

Mechanical properties of the textiles after the nanoparticle treatments

The major mechanical testing results are listed in Table 3. The table shows that adding different concentrations (0.15 wt%, 0.30 wt%, 0.60 wt%) of NP1, tear resistance and abrasion resistance were improved approximately by 56% and 100%, respectively. The mechanical testing results show that the increment of NP1 content does not significantly affect the mechanical properties. Higher curing temperature (145 °C compared with 140 °C) results in the deterioration of tear resistance of the control samples, but minor effect on the NP1 treated samples. However, the NP1 treatment slightly lowers down the dry recovery angle (for example, when curing at 140 °C, 0.6 wt% NP1 treatment resulted in 4° dry recovery angle decrease). This decrease may be the result of the unwelcomed inter-connection of the cotton fiber with the nanoparticle lumps in some parts [34]. Further raising the NP1 amount decreases the hand feel and wrinkle resistant property because of more aggregated sites of the nanoparticles. Besides these three concentrations, we also tested NP1 content treatment below 0.15 wt%, but the results were not very consistent, due to of the low nanoparticle adsorption efficiency during the dipping process [16].

Conclusions

In summary, we synthesized a positively charged vinyl group-based copolymer nanoparticle (NP1) via seeded radical polymerization, and allowed the nanoparticles to penetrate throughout a typical tightly woven fiber network. They formed a uniform nanofilm at the surface and experienced a phase-transition process and covalently bonded to the textile substrate. The nanofilm has low thickness (lower than 50 nm) and high homogeneity. Although there is only negligible amount of the nanoparticles applied (i.e. 0.15 wt%), there was a significant improvement of tearing (56%) and abrasion (100%) resistance for the substrate material. As a major concern in DP industry, the coating material demonstrated here significantly enhanced the desired properties of the substrate fabric. Since the properties and performances of the coating materials can deviate radically by selecting a large pool of vinyl monomers according to the proposed requirements of the currently available fabric materials, this work illustrates a new solution for achieving advanced performances of natural materials.

Acknowledgements This research work was partially supported by ITF (Hong Kong) grant No. 109.

References

1. Mahltig B, Böttcher H (2003) J Sol-Gel Sci Technol 27:43
2. Mahltig B, Fiedler D, Böttcher H (2004) J Sol-Gel Sci Technol 32:219
3. Vince J, Orel B, Vilcnik A, Fir M, Surca Vuk A, Jovanovski V, Simoncic B (2006) Langmuir 22:6489
4. Qian L, Sun G (2005) Ind Eng Chem Res 44:852
5. Hoefnagels HF, Wu D, de With G, Ming W (2007) Langmuir 23:13158
6. Service RF (2003) Science 301:909
7. Tiller JC, Liao CJ, Kim L, Klibanov AM (2001) Proc Natl Acad Sci 98:5981
8. Schramm C, Binder WH, Tessadri R (2004) J Sol-Gel Sci Technol 29:155
9. Mahltig B, Haufe H, Böttcher H (2005) J Mater Chem 15:4385
10. Mahltig B, Audenaert F, Böttcher H (2005) J Sol-Gel Sci Technol 34:103

11. Salon M-CB, Abdelmouleh M, Boufi S, Belgacem MN, Gandini A (2005) J Colloid Interface Sci 289:249
12. Soane DS, Offord DA, Linford MR, Millward DB, Ware W, Erskine L, Green E, Lau R (2003) US Pat Appl Publ US 2003013369, 2003
13. Alince B (2005) J Appl Polym Sci 98:1879
14. Alince B, Arnoldova P, Frolik R (2000) J Appl Polym Sci 76:1677
15. Zhang Y, Yang WL, Wang CC, Wu W, Fu SK (2006) J Nanosci Nanotechnol 6:2896
16. Yang C (2007) Explorations in the application of nanotechnology to improve the mechanical properties of composite materials, in "Chemistry", The Hong Kong University of Science and Technology, Hong Kong, p 161
17. PeulaGarcia JM, HidalgoAlvarez R, delasNieves FJ (1997) Colloid Surf A 127:19
18. Tsuruta LR, Lessa MM, Carmonaribeiro AM (1995) J Colloid Interface Sci 175:470
19. Goldfinger G (1969) Clean surfaces: their preparation and characterization for interfacial studies. Dekker, New York
20. Young RA, Rowell RM (1986) Cellulose: structure, modification, and hydrolysis. Wiley, New York
21. Pizarro GDC, Jeria M, Marambio OG, Huerta M, Rivas BL (2005) J Appl Polym Sci 98:1903
22. Isik B, Guenay Y (2004) Colloid Polym Sci 287:693
23. Kawaguchi H, Sugi Y, Ohtsuka Y (1981) J Appl Polym Sci 26:1649
24. Yan CE, Xu ZH, Cheng SY, Feng LX (1998) J Appl Polym Sci 68:969
25. Kim JH, Chainey M, El-Aasser MS, Vanderhoff JW (1989) J Polym Sci Polym Chem 27:3187
26. Kim JH, Chainey M, El-Aasser MS, Vanderhoff JW (1992) J Polym Sci Polym Chem 30:171
27. Frick JG, Kottes BH, Reid JD (1959) Text Res J 29:314
28. American Society for Testing and Materials (1969) Book of ASTM standards. American Society for Testing and Materials, Philadelphia, p 1716
29. American Society for Testing and Materials (1969) Book of ASTM standards. American Society for Testing and Materials, Philadelphia, p 539
30. Andersson M, Hietala S, Tenhu H, Maunu SL (2006) Colloid Polym Sci 284:1255
31. Hearle JWS (1963) J Appl Polym Sci 7:1207
32. Hearle JWS (1985) Cell Chem Appl 480
33. Hearle JWS, Sparrow JT (1971) Text Res J 41:736
34. Hearle JWS, Wilkins AH (2006) J Text Inst 97:1